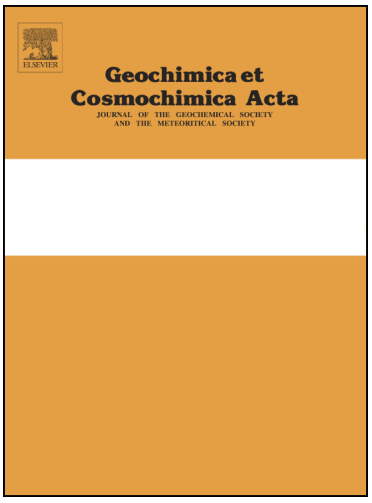

CO_2-dependent carbon isotope fractionation in Archaea, Part I: Modeling the 3HP/4HB pathway

Ann Pearson, Sarah J. Hurley, Felix J. Elling, Elise B. Wilkes

PII: S0016-7037(19)30391-6
DOI: https://doi.org/10.1016/j.gca.2019.06.042
Reference: GCA 11313

To appear in: *Geochimica et Cosmochimica Acta*

Received Date: 23 December 2018
Revised Date: 29 May 2019
Accepted Date: 19 June 2019

Please cite this article as: Pearson, A., Hurley, S.J., Elling, F.J., Wilkes, E.B., CO_2-dependent carbon isotope fractionation in Archaea, Part I: Modeling the 3HP/4HB pathway, *Geochimica et Cosmochimica Acta* (2019), doi: https://doi.org/10.1016/j.gca.2019.06.042

CO_2-dependent carbon isotope fractionation in Archaea, Part I: Modeling the 3HP/4HB pathway

Ann Pearson[1*], Sarah J. Hurley[1,2], Felix J. Elling[1], Elise B. Wilkes[1,3]

1. Department of Earth and Planetary Sciences, Harvard University, Cambridge MA 02138 USA
2. Department of Geosciences, University of Colorado, Boulder CO 80309 USA
3. Division of Geological and Planetary Sciences, California Institute of Technology, Pasadena CA 91125 USA

ABSTRACT

The 3-hydroxypropionate/4-hydroxybutyrate (3HP/4HB) pathway of carbon fixation is found in thermophilic Crenarchaeota of the order Sulfolobales and in aerobic, ammonia-oxidizing Thaumarchaeota. Unlike all other known autotrophic carbon metabolisms, this pathway exclusively uses HCO_3^- rather than CO_2 as the substrate for carbon fixation. Biomass produced by the 3HB/4HP pathway is relatively ^{13}C-enriched compared to biomass fixed by other autotrophic pathways, with total biosynthetic isotope effects (ε_{Ar}) of *ca.* 3‰ in the Sulfolobales and *ca.* 20‰ in the Thaumarchaeota. Explanations for the difference between these values usually invoke the dual effects of thermophily and growth at low pH (low $[HCO_3^-]$) for the former group *vs.* mesophily and growth at pH > 7 (high $[HCO_3^-]$) for the latter group. Here we examine the model taxa *Metallosphaera sedula* and *Nitrosopumilus maritimus* using an isotope flux-balance model to argue that the primary cause of different ε_{Ar} values more likely is the presence of carbonic anhydrase in *M. sedula* and its corresponding absence in *N. maritimus*. The results suggest that the pool of HCO_3^- inside *N. maritimus* is out of isotopic equilibrium with CO_2 and that the organism imports < 10% HCO_3^- from the extracellular environment. If correct and generalizable, the aerobic, ammonia-oxidizing marine Thaumarchaeota are dependent on passive CO_2 uptake and a slow rate of intracellular conversion to HCO_3^-. Values of ε_{Ar} should therefore vary in response to growth rate (μ) and CO_2 availability, analogous to eukaryotic algae, but in the opposite direction: ε_{Ar} becomes smaller as $[CO_{2(aq)}]$ increases and/or μ decreases. Such an idea represents a testable hypothesis, both in the laboratory and in natural systems. Sensitivity to μ and CO_2 implies that measurements of ε_{Ar} may hold promise as a pCO_2 paleobarometer.

1. INTRODUCTION

Three new pathways of carbon fixation have been discovered in recent decades: the 3-hydroxypropionate (3HP) cycle of Chloroflexi (Strauss and Fuchs, 1993), the 3HP/4HB cycle of Archaea (Berg et al., 2007; Könneke et al., 2014), and the dicarboxylic/4-HB (Di/4HB) cycle of Archaea (Huber et al., 2008). These three, plus the globally dominant Calvin-Benson-Bassham pathway (Calvin and Benson, 1948), the reverse tricarboxylic acid (rTCA) cycle (Evans et al., 1966), and the Wood-Ljungdahl, or Acetyl-CoA, pathway (*e.g.*, Wood et al., 1986) represent current knowledge of microbial autotrophy.

The rTCA, 3HP, 3HP/4HP, and Di/4HB pathways share the common property of being catalytic cycles in which one or more of the carbon-fixing enzymes is specific for HCO_3^- as a substrate. The biomass of organisms containing these pathways is enriched in ^{13}C (has higher values of $\delta^{13}C$) relative to biomass produced via the CBB and Acetyl-CoA pathways (Sirevag et al., 1977; Holo and Sirevag, 1986; van der Meer et al., 2001a, 2001b; House et al., 2003; van der Meer et al., 2003; Könneke et al., 2012; Jennings et al., 2014). Such organism-level biosynthetic isotope effects, or ε values, reflect the difference between total dissolved inorganic carbon (DIC) and the resulting biomass, and are reported as $\varepsilon \approx \Delta\delta = \delta^{13}C_{DIC} - \delta^{13}C_{biomass}$ (Hayes, 1993; 2001). The $\delta^{13}C$ characteristics of this family of autotrophic pathways reflect both the enrichment of ^{13}C in HCO_3^- when in equilibrium with CO_2 (Mook et al., 1974), plus the small (2-3‰) kinetic isotope effect (KIE) associated with enzymes specific for HCO_3^- (O'Leary et al., 1981; McNevin et al., 2006). Here we specify ε_{Ar} to mean the ε value for biomass of Archaea using the 3HP/4HB pathway.

The *ca.* 20‰ value of ε_{Ar} for marine 3HP/4HB Thaumarchaeota, specifically the model organism *N. maritimus* (Könneke et al., 2005; Könneke et al., 2012), is markedly different from the *ca.* 3‰ value for the 3HP/4HB Sulfolobales (van der Meer et al., 2001a ; House et al., 2003; Jennings et al., 2014). Genomic (Walker et al., 2010) and enzymatic (Könneke et al., 2014) evidence verify the 3HP/4HB metabolism in *N. maritimus* – *i.e.*, it contains a single carbon-fixing enzyme known to be solely dependent on HCO_3^-, not CO_2 – yet isotopically, it is distinct.

The marked difference in ε_{Ar} values between thermoacidophilic Sulfolobales and the ammonia-oxidizing marine Thaumarchaeota is well recognized (*e.g.*, Könneke et al., 2012; 2014) but has not yet been quantitatively explained. Explanation of the 20‰ ε_{Ar} value in Thaumarchaeota generally invokes both

direct enzymatic fractionation during carbon fixation (Könneke et al., 2012) and fractional contributions to biomass from ^{13}C-depleted organic carbon, either by true mixotrophy or in communities that contain heterotrophs in addition to autotrophs (*e.g.*, Herndl et al., 2005; Ingalls et al., 2006; Pearson et al., 2016). However, recent work indicates that *N. maritimus* and other ammonia-oxidizing marine Thaumarchaeota do not assimilate organic carbon into biomass and lack genes to acquire inorganic carbon from organic substrates like urea (Walker et al., 2010; Santoro et al., 2015; Kim et al., 2016). Therefore the *ca.* 20‰ value of ε_{Ar} for *N. maritimus* in pure culture as determined by Könneke et al. (2012) must solely reflect autotrophy. By analogy, similar values of ε_{Ar} in the marine environment (Schouten et al., 2013; Pearson et al., 2016; Hurley et al., 2019) suggest dominantly autotrophic processes as well. If so, prior reports of mixo- or heterotrophy may be attributed to artifacts of sampling or analysis.

Here we seek to reconcile these issues by modeling ε_{Ar} for both the Thaumarchaeon, *N. maritimus* and the well-studied member of the thermoacidophilic Sulfolobales, *M. sedula.* The results suggest that the extent of intracellular inorganic carbon disequilibrium may be the critical factor determining ε_{Ar} values expressed by the 3HP/4HB cycle. Because the intracellular carbon budget depends on the supply of CO_2, ε_{Ar} should be sensitive to changes in the carbon budget and growth rate. Our accompanying Part II paper supports this idea, showing that ε_{Ar} as recorded in thaumarchaeal membrane lipids isolated from marine suspended particulate organic matter (POM) correlates significantly with the *in-situ* CO_2 concentration (Hurley et al., 2019).

2. ISOTOPE FLUX-BALANCE MODEL

We constructed a carbon isotope and flux-balance model for bulk cellular carbon resulting from HCO_3^- fixation in the 3HP/4HB cycle (Figure 1). The model follows established principles (*e.g.*, Hayes, 2001; Tang et al., 2017) for interrogating stable isotope distributions in open systems and assumes steady state. Fluxes (φ) and kinetic isotope effects (KIEs, ε) are combined in a system of dependent linear equations of the form:

$$(1) \qquad \frac{\partial}{\partial t}\left(X_i\right) = \sum_j \varphi_j = 0; \qquad \frac{\partial}{\partial t}\left(\delta_{X_i}\right) = \sum_j \varphi_j \left(\delta_i - \varepsilon_j\right) = 0 \ ,$$

where X_i is the fraction of carbon in pool i, φ_j are the fluxes between i and other pools, and ε_j are KIEs specific to each of these fluxes.

The model can be applied to any 3HP/4HB organism for which carbon fixation rates, enzyme kinetic parameters, and KIEs are known or can be reasonably approximated. The simplified version (Figure 1a) is solved analytically, while the full model (Figure 1b) is implemented in Matlab V.R2015b and solved using differential equation integrator ODE23s.

2.1. Model inputs

Known biological and isotopic parameters for *M. sedula* and *N. maritimus* were compiled from the literature (Table 1) with the specific goal to explain the isotopic results of van der Meer et al. (2001a) for *M. sedula* and Könneke et al. (2012) for *N. maritimus*. Unknown values were estimated, either by analogy to related organisms or processes, or were calculated to achieve flux balance. References for all values are listed in the table, with additional parameters and details provided in Table S1 and Supporting Information.

M. sedula is an aerobic, hyperthermoacidophilic, coccoid organism of approximately 1 μm diameter, capable of autotrophic and heterotrophic growth (Huber et al., 1989; Auernik and Kelly, 2010); here we only model autotrophy under the conditions used by van der Meer et al. (2001a). *N. maritimus* is an aerobic, obligately autotrophic, rod-shaped cell of approximately 0.2 x 0.7 μm size that grows optimally in 28°C artificial seawater (Könneke et al., 2005; and additional references, Table 1).

Carbon fixation in the 3HP/4HB cycle is performed by a single, promiscuous enzyme that acts both as an acetyl-CoA carboxylase and a propionyl-CoA carboxylase (ACC; Menendez et al., 1999; Hügler et al., 2003). For *M. sedula*, activity of this enzyme has been studied *in vivo*, *in vitro*, and through heterologous expression in *Pyrococcus furiosus* (Hügler et al., 2003; Estelmann et al., 2011; Lian et al., 2016; Loder et al., 2016), collectively determining the ACC properties shown in Table 1. The kinetic properties of ACC in *N. maritimus* have proven difficult to characterize *in vitro* due to apparent instability of the complex (Könneke et al., 2014), so the values in Table 1 are derived from *in vivo* carbon fixation rate data and total cellular carbon content (Könneke et al., 2014; Hurley et al., 2016). The ACC-catalyzed reaction involves enolate attack on HCO_3^- in a mechanism analogous to phosphoenolpyruvate (PEPC) carboxylase for which

the KIE is well known (O'Leary et al., 1981; O'Leary, 1982; McNevin et al., 2006). We therefore adopt the KIE of PEPC for ε_{fix} in both taxa (Table 1).

Behavior of the model depends critically on the rate of intracellular hydration (and/or hydroxylation) of CO_2 to HCO_3^-. The distribution of carbonic anhydrase (CA) in the archaeal TACK superphylum (Guy and Ettema, 2011) was determined from GenBank BLASTP (Altschul et al., 1997) searches of α, β, γ, δ, ζ/η, and θ CAs (Smith et al., 1999) as detailed in Table S2. The statistical cutoff for a positive detection was set conservatively to $E < 10^{-3}$. These searches detected β-CA and γ-CA homologs in *M. sedula* and other 3HP/4HB Sulfolobales (*e.g.*, *Acidianus* spp.), and γ-CA homologs in 3HP/4HB Thaumarchaeota of the soil group (I.1b, *e.g.*, *Nitrososphaera viennensis*; Tourna et al., 2011) but none in *Nitrosopumilus* spp or other marine strains. Studies on the catalytic activity of the β and γ-CAs in *M. sedula* indicate that only the β-CA is active, while the γ-CA is inactive or serves another function (Auernik and Kelly, 2010; Lian et al., 2016). Regardless, *N. maritimus* contains neither option. In marine Thaumarchaeota, the conversion of CO_2 to HCO_3^- may be enzymatic via an unknown enzyme or result from non-enzymatic catalysis (Keller et al., 2015). It is unlikely to be purely abiotic, as the spontaneous hydration of CO_2 is kinetically very slow, *ca*. 10^6 slower than a typical CA (Bundy, 1986; Hopkinson et al., 2011) and 10^2-10^3 slower than needed to support carbon fixation in *N. maritimus*. We therefore postulate a biologically-mediated but slower process and consider its kinetics to behave as though governed by enzymatic catalysis; the process is labeled HYD, with isotope effect ε_{HYD}.

2.2. Model calculations

Solutions to the simplified model (Figure 1a) are calculated analytically as follows. Biomass production and $\delta^{13}C_{biomass}$ ($\delta_{biomass}$) depend on the measured carbon fixation rate (*fix*; Table 1), which is the product of biomass density (ρ) and growth rate (μ). This also equals the product of the biomass density, fractional protein content (γ), and the carbon fixation activity (A).

(2) $$fix = \mu\rho = \rho\gamma A .$$

The flux of $CO_2 \rightarrow HCO_3^-$ (φ_4) depends on the hydration rate of CO_2, either by CA or by HYD, and is solved assuming the process is governed by Michaelis-Menten kinetics:

$$\varphi_4 = \frac{k_{cat1} E_1 C_e}{\left(K_{M1} + C_e\right)}. \quad (3)$$

Here, C_e (extracellular CO_2 concentration) is known from culture conditions, and the K_{M1} and k_{cat1} values of CA in *M. sedula* are conservatively based on the slowest CAs of Archaea (Smith and Ferry, 2000) and on expression of the β-CA of *M. sedula* in *P. furiosus* (Lian et al., 2016). Values of K_{M1} and k_{cat1} for the HYD process in *N. maritimus* are modeled to achieve flux and isotope balance at steady state. The dehydration flux (φ_5) is determined by mass balance, also defining the critical backflow ratio, *B*:

$$\varphi_5 = \varphi_4 - fix, \text{ and } B = \frac{\varphi_5}{\varphi_4}. \quad (4)$$

C_i (intracellular CO_2 concentration) and δ_{Ci} ($\delta^{13}C$ value of intracellular CO_2) are taken to be equal to C_e and δ_{Ce} based on calculations of CO_2 diffusion through spherical and cylindrical shapes with a consumption flux at the central axis (Supporting Information; Zeebe and Wolf-Gladrow, 2001; McMurtrey, 2016). H_i (intracellular HCO_3^- concentration) is determined from the enzyme kinetics of ACC as published in Hügler et al. (2003) for *M. sedula* and as estimated from related work for *N. maritimus* (Martens-Habbena et al., 2009; Könneke et al., 2014) (Table 1). Cells are assumed to be 80% protein ($\gamma = 0.8$), and the amount of this cell protein that is devoted to carbon fixation (ACC abundance, E_{fix}) is set at 2% in the faster-growing *M. sedula* and 1% in the slower-growing *N. maritimus*. The 2% value for *M. sedula* is known experimentally (Hügler et al., 2003; Loder et al., 2016), while the 1% *N. maritimus* value is consistent with proteomics data (Qin et al., 2018). Values for K_{M2} and k_{cat2} are known for ACC in *M. sedula* and are adjusted by an order of magnitude for *N. maritimus* to reflect growth behavior (Table 1; and Discussion). By rearrangement of the Michaelis-Menten equation, these parameters are combined to solve for H_i at steady state:

$$H_i = \frac{fix K_{M2}}{\left(k_{cat2} E_{fix} - fix\right)}. \quad (5)$$

The carbon isotope ratios δ_{Hi} and δ_{Ar} then are determined by isotope balance around H_i:

$$(6) \qquad \delta_{H_i} = \frac{\varphi_4(\delta_{C_e} - \varepsilon_{HYD}) + \varphi_5(\varepsilon_{HYD} + 1000(1-\alpha)) + fix\varepsilon_{fix}}{\varphi_4}; \quad \delta_{biomass} = \delta_{H_i} - \varepsilon_{fix}.$$

Finally, ε_{Ar} is calculated relative to external HCO_3^- (δ_{H_e}) according to the exact formula (Eq. 7) rather than the $\varepsilon_{Ar} \approx \delta^{13}C_{DIC} - \delta^{13}C_{biomass}$ approximation:

$$(7) \qquad \varepsilon_{Ar} = 1000\left[\frac{(\delta_{H_e} + 1000)}{(\delta_{biomass} + 1000)} - 1\right].$$

To simulate a cell that also invests energy in HCO_3^- import and/or has the capacity to incorporate carbon from organic sources, specifically as metabolic CO_2 (*e.g.*, from urea lysis), equations for a Matlab-enabled numerical model that includes φ_3, φ_6, and φ_7 (Figure 1b) are presented in Supporting Information.

3. RESULTS

3.1. Simplified model, *M. sedula*

The predicted flux balances for *M. sedula* and *N. maritimus* are notably different in their magnitude of intracellular conversion between CO_2 and HCO_3^- (Figure 2a). When normalized to carbon fixation rate (*i.e.*, $fix \equiv 1$), the hydration flux (φ_4) for *M. sedula* is nearly 200-fold faster than for *N. maritimus*, resulting in dehydration backflow (B) ratios >> 0.99 *vs.* ≤ 0.47, respectively (Table 1).

Rapid exchange of DIC species within *M. sedula* has isotopic consequences, namely, that H_i and C_i are predicted to approach isotopic equilibrium intracellularly (Figure 2b). This implies that δ_{Hi} becomes equal to δ_{He}, regardless of the extent of active HCO_3^- import (unlikely at pH 2, but isotopically inconsequential even if present). The only expressed KIE affecting ε_{Ar} is therefore the magnitude of ε_{fix}, implying that $\delta_{biomass}$ should be 2.5‰ more negative than δ_{He} (or 2.5‰ more positive than δ_{Ce}, given $\alpha_{CO2\text{-}HCO3^-} = 0.995$ at 65°C; Table S1; Figure 2b). The modeled value for $\delta_{biomass}$ is within the reported error (0.4‰) of the *M. sedula* experiment of van der Meer et al. (2001a) (Table 1), indicating that the choice to make ε_{fix} equal to the KIE of PEPC is a reasonable one. Importantly, our model result is based on minimal assumptions, as the carbon isotope and concentration parameters were taken directly from the data of van

der Meer et al. (2001a), the carbon-fixing ACC enzyme has been studied extensively (*e.g.*, Hügler et al., 2003), and the CA properties are conservative estimates (*i.e.*, the slowest possible supply of HCO_3^-) based on experimental results from other Archaea (Smith and Ferry, 2000). The model indicates that when CO_2 is abundant, CA readily supplies isotopically-equilibrated intracellular HCO_3^- for carbon fixation, and the overall biosynthetic isotope effect ε_{Ar} should be a small value approximately equal to ε_{fix} (Figure 2b).

3.2. Simplified model, *N. maritimus*

Carbon isotope fractionation in *N. maritimus* depends on the kinetics of CO_2 diffusion into/out of the cell, conversion of the intracellular pool of CO_2 to HCO_3^-, and subsequent fixation of this HCO_3^- into biomass. This implies that ε_{Ar} values for *N. maritimus* are strongly dependent on the interplay between the hydration flux (φ_4, dependent on properties of the hypothesized enzyme, HYD) and its KIE (ε_{HYD}). Spontaneous hydration of CO_2 to HCO_3^- is very slow, with an apparent first-order rate constant of 0.04 s^{-1} for combined hydration and hydroxylation (at 25°C, pH 7.5; Zeebe and Wolf-Gladrow, 2001). At a maximum 50 μM CO_2 concentration experienced by *N. maritimus* and a mean carbon fixation rate of 3×10^{-6} fmolC $cell^{-1}$ s^{-1}, the non-catalyzed HCO_3^- yield would be only 3×10^{-8} fmolC $cell^{-1}$ s^{-1}, which is 1% of the needed flux. It therefore appears that the intracellular production of HCO_3^- in *N. maritimus* must be enzymatically-mediated, either by a dedicated enzyme or as a non-specific side reaction of another process. Here we call that process HYD and model it with Michaelis-Menten kinetics.

When the KIE for CO_2 hydration by HYD is set to 25‰ (Zeebe, 2014), the model yields a backflow ratio B of 0.47 (Figure 2c,d). Conversely, the KIE of the hydration reaction as mediated by CA (1‰; Paneth and O'Leary, 1985) would not be an allowed solution, as it would result in a maximum 10‰ value of ε_{Ar}, which is smaller than the observed ε_{Ar} value of *ca.* 20‰ for *N. maritimus*. The model therefore limits ε_{HYD} to values between 11‰ (at B approaching 0; grey circle, Figure 2d) and 25‰ (at B = 0.47; black circle, Figure 2d). For simplicity we discuss only the solution using ε_{HYD} = 25‰ but recognize that this estimate is highly uncertain and a critical area for future experimental study.

The model for *N. maritimus* indicates that because $B < 1$, the two HCO_3^- pools, H_i and H_e, cannot be in equilibrium, and $\delta_{Hi} \neq \delta_{He}$ (Table 1; Figure 2c). If it is valid to assume that ε_{fix} is equal to the KIE for

PEPC (consistent with the *M. sedula* results) then such a result is obvious: δ_{Hi} cannot exceed $\delta_{biomass}$ by more than the value of ε_{fix}, and therefore δ_{Hi} must be < δ_{He} (Figure 2c). Most importantly, ε_{Ar} is predicted to depend on the balance between the hydration flux (φ_4) and the fixation rate (*fix*), because these two parameters together determine the backflux ratio (Eq. 4; Figure 2d). The value of *fix* depends on μ (Eq. 2), because ρ is assumed to be constant, while φ_4 depends on C_e (Eq. 3). This implies that the magnitude of ε_{Ar} should depend directly on the ratio of μ to C_e. Algebraic rearrangement (derivation in Supplemental Information) simplifies this dependence to an equation similar to the alkenone paleobarometer (Jasper et al., 1994), here with the biological term 'β' explicitly defined in terms of kinetic and other physiological properties (Eq. 8, 9). The solution for Eq. (8), combined with Eq. (7), yields ε_{Ar} as a function of μ and $CO_{2(aq)}$:

$$\varepsilon_{Ar} \approx \Delta\delta = \delta_{H_e} - \delta_{biomass} = \varepsilon_{fix} - \beta\left(\frac{1}{C_e} + \frac{1}{K_{M1}}\right), \text{ where} \tag{8}$$

$$\beta = \mu\left(\frac{\rho\varepsilon_{net}K_{M1}}{k_{cat1}E_1}\right), \text{ and } \varepsilon_{net} = \varepsilon_{fix} - \varepsilon_{HYD} - 1000(1-\alpha). \tag{9}$$

The value of β controls the sensitivity of ε_{Ar} to μ, while the overall sensitivity of ε_{Ar} to C_e is modulated by the assumed value of the kinetic parameter K_{M1}.

3.3. Sensitivity analysis

3.3.1. N. maritimus

To explore the potential response of ε_{Ar} to variations in seawater chemistry, we modeled the predicted range of ε_{Ar} over C_e conditions typical of seawater and using growth rates for cultivated marine Thaumarchaeota (range of reported doubling times for cultivated isolates is 21 to > 120 h; Könneke et al., 2005; Qin et al., 2014; Santoro et al., 2011; Figure 3). Although the specific values for the enzyme-dependent components of β remain uncertain, the example shown here illustrates the potential for further refinement of a pCO_2 proxy if (*i*) ε_{Ar} can be calibrated experimentally and (*ii*) the total ammonia-oxidizing,

marine Thaumarchaeota community has a similar CO_2 sensitivity as *N. maritimus*. Values of ε_{Ar} become larger as [$CO_{2(aq)}$] becomes smaller, *e.g.*, in the surface ocean relative to the mesopelagic. Similarly, we would predict ε_{Ar} to be larger during glacial periods relative to interglacial periods due to lower CO_2 content of the ocean-atmosphere system during glacial intervals. Initial data from a cruise in the Atlantic Ocean were used to tune the model to reflect the observed response of ε_{Ar} to *in-situ* [$CO_{2(aq)}$] (see the Part II companion paper to this work; Hurley et al., *submitted*), again analogous to strategies taken for alkenone paleobarometry (Rau et al., 1992; Bidigare et al., 1997, Laws et al., 2001). Both the model and the Atlantic Ocean data indicate the full range of ε_{Ar} is relatively small. Here we hypothesize a range of < 5‰ between typical surface and deep ocean conditions (Figure 3), which also is consistent with existing $\delta^{13}C$ data for sedimentary biphytanes (Schouten et al., 2013) and glycerol dialkyl glycerol tetraethers (GDGTs; Pearson et al., 2016).

3.3.2. M. sedula

An analogous sensitivity analysis for *M. sedula*, calculating the expected range of ε_{Ar} as a function of experimental C_e values (7-50% $CO_2(g)$ at 250-300 kPa; Menendez et al., 1999; van der Meer et al., 2001a; Auernik and Kelly, 2010) and growth rates (T_d = 4 to 15 hr; Auernik and Kelly, 2010; Estelmann et al., 2011), indicates the expressed fractionation should be nearly invariable (Supplemental Figure S2). Values of ε_{Ar} would be < 3‰ at all [$CO_{2(aq)}$] concentrations > 1 mM, equivalent to > 2.5% $CO_2(g)$ in the headspace. This is consistent with the small difference in observed ε_{Ar} values between the studies of van der Meer et al. (2001a) and House et al. (2003), despite their differences in $CO_2(g)$ pressure.

3.4. *N. maritimus* numerical model including urea and bicarbonate fluxes

The above results assume that no carbon is assimilated directly from HCO_3^- or derived from respiration (including urea metabolism). Using the full numerical model (Figure 1b), we simulated active import of HCO_3^- (H_e) by *N. maritimus* equivalent to 0, 10, or 20% of total carbon fixation (*fix*) (Figure 4). Uptake of H_e produces a large decrease in the magnitude of ε_{Ar}, because it contributes ^{13}C-enriched carbon (δ_{He}) directly to the H_i pool used for carbon fixation. For example, with H_e import equivalent to 20% of the

cellular carbon budget, the resulting values of ε_{Ar} generally would be < 18‰, a value that has not been observed to date for *N. maritimus* (Könneke et al., 2012). However, at slower growth rates and low C_e conditions, import of up to 10% HCO_3^- would have a small (~1‰) effect on ε_{Ar} and could be accommodated. This suggests that in general *N. maritimus* actively imports little to no HCO_3^-, *i.e.*, it does not invest in this energy-requiring process. Thaumarchaeota genomes do not appear to encode any ATP-dependent active uptake systems for HCO_3^-, but some representatives of the marine group I.1a division which includes *N. maritimus* do have an electrochemical potential-driven Na^+/HCO_3^- transporter (Offre et al., 2014; Santoro et al., 2015). However, transcriptomic and proteomic data indicate the gene product for this transporter in *N. maritimus* (Nmar_0485) is minimally detected, comprising fractionally $3e^{-6}$ and $3e^{-5}$ of the total signal in the transcriptome and proteome, respectively (Qin et al., 2018). Bicarbonate ion pumping may therefore remain largely unutilized (≤ 10% of total carbon) in Thaumarchaeota that are already operating near the extremes of energy limitation (Valentine, 2007; Martens-Habbena et al., 2009), although this requires further investigation both in cultures and in natural populations.

Similarly, sources of metabolic CO_2 or the influence of urea uptake also are predicted to have little isotopic influence due to the rapid diffusional flux of CO_2 across the cell boundary (Figure 4). Diffusion mixes away the organic-derived CO_2 signal such that it affects ε_{Ar} by ≤ 0.5‰ even when increased to 60% of the net carbon flux. This would imply that cells could switch between ammonia and urea as nitrogen sources with minimal impact on ε_{Ar}. Our model does not address direct assimilation of organic metabolites such as succinate or pyruvate into biomass, as currently there is no evidence that cultured taxa of marine Thaumarchaeota incorporate these substrates (Kim et al., 2016; Dekas et al., 2018).

4. DISCUSSION

4.1. Physiological and evolutionary role of the 3HP/4HB pathway

Growth under conditions of extreme resource limitation is thought to be a common feature not only of the Archaea, but of Earth's microbial biosphere in general (Valentine, 2007; Lever et al., 2015). While typically discussed in the context of energy limitation, here we argue that in the case of marine Thaumarchaeota, carbon limitation also likely plays an important role in their physiology, due to the

apparent absence of a functional CA. The ammonia-oxidizing, marine Thaumarchaeota have a low maintenance energy demand and can grow at < 10 nM ammonia concentration (Martens-Habbena et al., 2009). Slow growth rates and small cell sizes imply that they have maximum carbon assimilation rates estimated to be 8×10^{-6} fmolC $cell^{-1}$ s^{-1} (Könneke et al., 2005; Könneke et al., 2014; Hurley et al., 2016; Table 1). This is nearly 4000 times slower than the upper range of carbon fixation rates per cell in large marine cyanobacteria (*i.e.*, photoautotrophs employing the CBB pathway) (Klawonn et al., 2016). Thaumarchaeal optimization to minimum energy and carbon fluxes contrasts with the aerobic, thermoacidophilic Sulfolobales, who occupy specific niche conditions around pH 2-3 and 75°C in continental hot springs and whose growth may be optimized for specific electron donor/acceptor pairs to the exclusion of other available higher-energy-yielding reactions (Amenabar et al., 2017). These differing energetic and substrate pressures have implications for the evolutionary history and physiological function of the 3HP/4HB pathway in the two groups.

4.1.1. Evolutionary history and environmental pressures

Analyses of whole genomes and specific genes indicate that the phyla Thaumarchaeota (Spang et al., 2010; Pester et al., 2011) and Crenarchaeota are part of a clade known as the TACK superphylum (Guy and Ettema, 2011; Hug et al., 2016). The phylogenetic placement of the TACK group within the archaeal domain remains debated, including whether it is ancestral to or descended from within Euryarchaeota (Adam et al., 2017; Williams et al., 2017).

The 3HP/4HB pathway is found in the aerobic, ammonia-oxidizing Thaumarchaeota, specifically groups I.1a and I.1b (Hallam et al., 2006; Walker et al., 2010; Stieglmeier et al., 2014). Other taxonomic divisions of Thaumarchaeota (*e.g.*, I.1c, I.1d) are organotrophic, can grow anaerobically, and do not contain genes for ammonia oxidation or carbon fixation (*c.f.*, Adam et al., 2017). This suggests that ammonia oxidation and the 3HP/4HB pathway are not ancestral characteristics of the phylum Thaumarchaeota. Similarly, although several aerobic genera of the Sulfolobales contain the 3HP/4HB pathway, their sister lineage, the anaerobic *Desulfurococcales,* contains the similar and possibly ancestral Di/4HB carbon fixation pathway (Huber et al., 2008), as do the more deeply branching *Thermoproteales* (Berg et al., 2010).

This implies that the 3HP/4HB pathway also is not an ancestral character of the Crenarchaeota. Given its simplicity, as well as differences between 3HP/4HB Sulfolobales and 3HP/4HB Thaumarchaeota in some of the enzymatic steps downstream from ACC, the pathway is believed to have evolved independently in the two phyla (Könneke et al., 2014). Phylogenetic analyses confirm this idea, showing that the origins of several key enzymes downstream from ACC in the 3HP/4HB pathway of Thaumarchaeota are different from the functionally-equivalent versions in Sulfolobales (Berg et al., 2007; Könneke et al., 2014).

Instead, the common feature of autotrophic Archaea appears to be production of the simple metabolic building block, acetyl-CoA (Berg et al., 2010). Intracellular cycles based on acetyl-CoA production may be the ancestral state of Archaea, while the range of strategies to produce acetyl-CoA reflects the environmental pressures as Archaea diversified. For example, while the Di/4HB pathway in *Desulfurococcales* is oxygen sensitive (Huber et al., 2008), the enzyme 4-hydroxybutyryl-CoA dehydratase – which is common to both Di/4HB and 3HP/4HB – has evolved to be non-oxygen-sensitive in both the 3HP/4HB Sulfolobales (Hawkins et al., 2014) and the ammonia-oxidizing Thaumarchaeota (Könneke et al., 2014). This suggests the 3HP/4HB pathway developed in tandem with niche adaptation to aerobic environments.

An additional feature distinguishing the 3HP/4HB pathway in ammonia-oxidizing Thaumarchaeota from the pathway in aerobic Sulfolobales is its lower energy requirement. The version in Sulfolobales requires 9 ATP molecules per unit of pyruvate produced, apparently more than either the CBB or 3HP pathway (7 ATP), or the Di/4HB pathway (5 ATP) (Berg et al., 2010); yet the 3HP/4HB pathway in Thaumarchaeota also has a low requirement of 5 ATP (Könneke et al., 2014). This feature is consistent with its apparently robust association with the low energy-yielding process of aerobic ammonia oxidation. Importantly, the concomitantly slow growth rates also imply that survival could be possible under very carbon substrate-limited conditions, as would be the case for cells requiring an internal pool of HCO_3^- that was being generated by a catalytically-slow process (*i.e.*, the hypothetical HYD enzyme). Slow growth and low carbon demand could permit HYD to compensate for the absence of functional CA among the Thaumarchaeota. Conversely, the development of the high ATP-requiring 3HP/4HB pathway in aerobic Sulfolobales may more strongly reflect selection for oxidative niche space within hot spring environments,

where the lower pH conditions effectively require investment in CA enzymes. These different physiological factors represent challenges to determining the evolutionary age of the 3HP/4HB pathway, including when its isotopic imprint may first appear in the geologic record.

4.1.2. Physiology and enzyme kinetics

The different origins of the 3HP/4HB pathway in Thaumarchaeota and Crenarchaeota are reflected in the properties of their enzymes for carbon fixation, consistent with the idea that enzymatic efficiency reflects environmental and evolutionary pressures (Albery and Knowles, 1976).

For our model, enzyme constants for *M. sedula* were taken directly from the literature, while those for *N. maritimus* were predicted by isotope flux balance (Table 1). The resulting catalytic properties, including for the hypothetical CO_2-hydrating enzyme, HYD, are within normal ranges (within 60%, or *ca.* 1σ, of the median) of cellular enzymatic systems (Bar-Even et al., 2011). For *M. sedula*, the observed efficiencies (k_{cat}/K_M) of 5×10^3 mM^{-1} s^{-1} and 90 mM^{-1} s^{-1} for CA and ACC, respectively, are within the 1σ range of the median efficiency for all known enzymes (10^2 mM^{-1} s^{-1}). For *N. maritimus*, the predicted values of 1×10^4 mM^{-1} s^{-1} and 9×10^3 mM^{-1} s^{-1} for HYD and ACC, respectively, are higher (*i.e.*, more efficient) but also still within normal ranges (Bar-Even et al., 2011).

These values appear to directly reflect the different substrate challenges experienced by the 3HP/4HB pathway in the two groups. Low intracellular concentrations of substrate (here, HCO_3^-) would depress K_M values (Bennett et al., 2009), consistent with the predicted 10-fold lower K_M for the ACC of *N. maritimus* relative to *M. sedula*. Although the 30 μM K_M value predicted for ACC in *N. maritimus* is below the global median K_M value for all enzymes (Bar-Evan et al., 2011), it is considerably higher than the *ca.* 100 nM K_M reported for ammonia oxidation (Martens-Habbena et al., 2009). This suggests that metabolic optimization for low substrate availability is a consistent feature of marine Thaumarchaeota, but that unknown factors may prevent further reduction of the K_M for ACC. Additional increases in efficiency for an enzyme in which K_M already has been minimized can only be achieved by increasing the rate of substrate turnover (k_{cat}). Correspondingly, the predicted k_{cat} for ACC in *N. maritimus* is faster than in *M. sedula* (Table 1). Overall, the ACC in *N. maritimus* appears to have evolved to be *ca*. 100-fold more efficient. In

tandem with a low ATP requirement, this is consistent with the energy-poor ecology and slow growth rates of all known isolates of marine Thaumarchaeota (*e.g.*, Könneke et al., 2005; Santoro et al., 2011).

Perhaps more interesting are the predicted properties of the unknown process, HYD, relative to the known catalytic properties of CA. Both β and γ-CAs are widespread in the Archaea and appear to have ancient origins, leading to the suggestion that early chemoautotrophic pathways may have been CA-dependent (Smith et al., 1999). Relatively fast catalytic rates and high K_M values are typical of scenarios in which the substrate is not limiting (*e.g.*, elevated CO_2 levels at pH 2-3). Catalytic properties of the β-CA of *M. sedula*, either purified from overexpression in *Escherichia coli* or engineered into *P. furiosus* (Lian et al., 2016), agree with those observed for β-CA of *Methanobacterium thermoautotrophicum* (k_{cat} = 1.7 $\times 10^4$ s^{-1}, K_M = 2.9 mM; Smith and Ferry, 1999) and are characteristic of high CO_2 conditions. The CAs in Archaea are similar in overall efficiency to the CAs of Bacteria and Eukarya (Smith and Ferry, 2000). Importantly for growth of *M. sedula*, its CA should yield abundant HCO_3^-, which is consistent with a low affinity (K_M = 300 μM) for its ACC (Table 1). For comparison, this is higher than all known K_M values for RuBisCO (for CO_2) (Tcherkez et al., 2006), implying that RuBisCO has evolved under greater carbon limitation than the ACC of *M. sedula*, and that accordingly, CA is a fundamental part of the 3HP/4HB pathway in aerobic Sulfolobales.

The opposite scenario emerges for the hypothetical HYD enzyme in *N. maritimus*. In this organism, the predicted efficiencies of HYD and ACC are nearly equal. This implies the two enzymes have experienced similar evolutionary pressures with respect to optimizing the rate of carbon fixation. The high substrate affinity (K_M = 3 μM) proposed for HYD would be consistent with the need to accommodate the low [$CO_{2(aq)}$] environment of seawater, while the catalytic rate would adjust to match the demand from ACC, assuming the overall rate of carbon fixation is limited by the availability of ATP and NADPH generated from ammonia oxidation. More critical is the question of the nature of the proposed HYD enzyme. No known β or γ-CAs are present in *N. maritimus* (Table S2), but other cellular processes may serve to hydrate CO_2. As one example, binding of CO_2 to free or exposed amino acids to form carbamino acids can release HCO_3^- during subsequent cleavage (Johnson and Morrison, 1972; Smith and Ferry, 2000). Understanding the rate and mechanism of intracellular HCO_3^- production is a critical need for future

physiological studies of marine (group I.1a) ammonia-oxidizing Thaumarchaeota, as is exploration of the physiology of HCO_3^- generation in the soil group I.1b in which there is an annotated γ-CA of unestablished function but which is proposed to be extracellular and facilitate CO_2 uptake rather than generate HCO_3^- (Kerou et al., 2016).

4.2. Prospects for paleobarometry

Several factors affect practical application of the ε_{Ar} model (Eq. 8, 9) to reconstruct past pCO_2 levels from the marine sedimentary record. Accurate paleobarometry requires that the signal be (*i*) preserved with high fidelity and recoverable from marine sediments, (*ii*) not compromised by metabolic or taxonomic heterogeneity in the water column or overprinted by sedimentary Archaea, (*iii*) have a large enough range in ε_{Ar} relative to analytical or other uncertainties to detect changes in dissolved CO_2 and therefore pCO_2 and (*iv*) reliably record the original values of $\delta_{biomass}$ in preserved archaeal lipid biomarkers. These issues are discussed briefly below, with additional discussion of the influence of water column properties appearing in the Part II paper (Hurley et al., 2019).

4.2.1. Archaeal lipid biomarkers

The GDGT lipids of Archaea can be recovered for isotopic analysis as membrane core lipids (Smittenberg et al., 2004; Ingalls et al., 2006; Shah et al., 2008; Pearson et al., 2016) or as their central hydrocarbon chains, known as biphytanes (*e.g.*, Hoefs et al., 1997; Kuypers et al., 2001; Pancost et al., 2008; Schoon et al., 2013). Current evidence indicates that values of δ_{GDGT} are equal to $\delta_{biomass}$ (Könneke et al., 2012) but that values of $\delta_{biphytane}$ are slightly depleted in ^{13}C relative to $\delta_{biomass}$, by perhaps 1‰ (Pearson et al., 2016). More systematic work is needed to precisely characterize $\delta^{13}C$ values of biphytanes, but both biphytanes and GDGTs potentially could be used as isotopic biomarkers in paleo-pCO_2 applications if adequate internal isotopic standards and other quality control criteria are specified.

4.2.2. Biosynthetic and community effects

Planktonic, rather than benthic, sources of archaeal biomass are thought to dominate the sedimentary record in most locations – an idea that is supported by key GDGT ratios such as TEX_{86} (Schouten et al., 2002), the [2/3] ratio (Taylor et al., 2013), and specific anomalous patterns that occur in the presence of benthic sources (*e.g.*, Pancost et al., 2001; Zhang et al., 2011). Good agreement between water-column and sedimentary carbon isotope data was apparent in early measurements of biphytanes (Hoefs et al., 1997), particularly for $\delta^{13}C$ values derived from the 5-ringed GDGT known as crenarchaeol, which appears to reflect planktonic sources only (*c.f.*, Schouten et al., 2013). The planktonic signature for crenarchaeol, as measured in its unique cyclohexane ring-containing $C_{40:3}$ biphytane, appears robust even in hydrate-bearing sediments, mud volcanoes, and other locations affected strongly by methane and other hydrocarbon seepage (Schubotz et al., 2011; Zhang et al., 2011). Values for $C_{40:3}$ biphytane retain a water column signature ($\delta^{13}C \geq$ -23‰) even when other biphytanes from identical samples record a methane-derived benthic signal (*e.g.*, $\delta^{13}C \leq$ -60‰). Further arguments against significant benthic overprinting of crenarchaeol include the slow apparent growth rates of Archaea in the deep biosphere (Xie et al., 2013), combined with high preservation potential of planktonic-derived GDGTs (Schouten et al., 2010; Lengger et al., 2014).

Of greater uncertainty is the question of direct organic carbon assimilation into biomass of marine planktonic Archaea, and specifically into their lipids. Early work indicated the potential for uptake of ^{3}H-labeled amino acids into Thaumarchaeota but did not determine if the associated carbon was assimilated (Ouverney and Fuhrman, 2000; Herndl et al., 2005). Conversely, a mesocosm incubation showed strong assimilation of inorganically-derived ^{13}C into archaeal lipids, although without an analogously ^{13}C-labeled organic control for comparison (Wuchter et al., 2003). Recently, significant uptake (into DNA) of ^{13}C-labeled acetate relative to ^{13}C-labeled inorganic carbon was observed in stable isotope probing (SIP) experiments targeting the TACK Archaea (Seyler et al., 2018). However, it is unclear how much the relatively short incubation times and lack of added electron donor (NH_4^+) to facilitate autotrophic growth may have enriched the total populations differently from natural communities.

In our own work, we previously have argued for *ca*. 20% direct organic carbon assimilation using a combination of natural radiocarbon ($\Delta^{14}C$) and $\delta^{13}C$ signatures in biphytanes and GDGTs (Pearson et al.,

2001; Ingalls et al., 2006; Pearson et al., 2016). Of the two types of carbon isotope data, $\Delta^{14}C$ has the larger signal and was reported to be statistically significant: a water column sample from 670 m depth was estimated to be 83% autotrophic and 17% heterotrophic, with 1σ uncertainty of ± 11% (Ingalls et al., 2006). Based on this result, the fraction of assimilated organic carbon, or mixotrophy, could be small, but is predicted to be > 0%. Mixotrophy also has been proposed for some taxa of cultivated Thaumarchaeota, including both from the soil group I.1b (Tourna et al., 2011) and some isolates of the marine group I.1a (Qin et al., 2014), which cannot grow unless supplemented with organic acids such as pyruvate or 2-oxoglutarate. However, recent experiments on the physiology of ammonia-oxidizing Thaumarchaeota indicate that these substrates function as free-radical scavengers to detoxify intermediates of ammonia oxidation and are not assimilated into biosynthetic products (Kim et al., 2016). Collectively, the data leave open the possibility that marine Thaumarchaeota are strict chemoautotrophs and that heterotrophy is significant only among the planktonic Euryarchaeota (Iverson et al., 2012). More work is required to examine this possibility using a variety of analytical approaches (*e.g.*, Dekas et al., 2018). Currently available $\delta^{13}C_{GDGT}$ data and resulting ε_{Ar} calculations are consistent with the range of values predicted by our strict autotrophy model (Eqs. 8, 9), in both the reported means of GDGTs and biphytanes (Schouten et al., 2013) as well as the specific isotopic values reported in recent studies that give emphasis to crenarchaeol as a planktonic thaumarchaeal biomarker (Pearson et al., 2016; Polik et al., 2018; Hurley et al., 2019).

4.2.3. Sensitivity of ε_{Ar} to variations in pCO_2

Proxy sensitivity will determine the quality of pCO_2 reconstructions obtained from Thaumarchaeota ε_{Ar} values. As currently modeled, the carbon isotope variation over reasonable marine CO_2 concentrations (*e.g.*, 10-50 μM) is expected to be ≤ 5‰ (Figure 3). For applications using $\delta^{13}C$ measurements of GDGT lipids, our recent work using spooling-wire micro-combustion IRMS (SWiM-IRMS; Sessions et al., 2005) has a demonstrated precision and accuracy of 0.2‰ (1σ) for crenarchaeol isolated from relatively small samples of sediments, *i.e.*, quantities that can be obtained from ocean drilling program core repositories (Pearson et al., 2016; Elling et al., *in revision*; Polik et al., 2018). When translated to uncertainty in $[CO_{2(aq)}]$ reconstructions, this analytical limitation alone implies that the ε_{Ar} proxy is

unlikely to be useful under conditions of atmospheric pCO_2 > 1500 ppm (Figure 5), implying it will be best suited to reconstruct episodes of Earth history in which the atmospheric CO_2 content was < 4 times the pre-anthropogenic Holocene level. This range of sensitivity could be particularly useful for tackling unresolved questions about Miocene-Pliocene atmospheric transitions (Foster et al., 2012; Zhang et al., 2013; Greenop et al., 2014) but it may be less useful for early Cenozoic greenhouse atmospheres that may have reached values of 2000 ppm (Royer et al., 2001; Pagani et al., 2005). For example, a relatively CO_2-insensitive or less-sensitive value of ε_{Ar} may be justifiably assumed for Eocene hyperthermals, with the associated benefit that any change in $\delta^{13}C$ values of crenarchaeol would closely reflect the change in total ocean ^{13}C inventory and $\delta^{13}C_{DIC}$ could be reconstructed (Elling et al., *in revision*). The same may apply to earlier Cretaceous records that also were suggested to reflect real change in the ^{13}C content of the ocean (Kuypers et al., 2001). Currently, no high-resolution temporal records exist for the Neogene, the primary period in which ε_{Ar} would be expected to have the most useful proxy sensitivity.

Finally, consistent with the predicted sensitivity threshold, existing lipid data from low-pH, high CO_2 cultures of *N. maritimus* yield values near the predicted lower range of ε_{Ar}, with no isotopic response when DIC concentrations are further increased (Könneke et al., 2012). Additional preliminary data from chemostat trials also show low values of ε_{Ar} with little apparent response to changes in growth rate, likely because $[CO_{2(aq)}]$ was *ca.* 40 μM in all experiments, which would be equivalent to seawater in equilibrium with a >1000 ppm pCO_2 atmosphere (Hurley et al., 2016; Supplemental Information, Figure S3). Additional experiments are required over a range of growth rates and at lower CO_2 conditions to rigorously calibrate the sensitivity of ε_{Ar} to μ and $[CO_{2(aq)}]$.

5. CONCLUSIONS

The flux-balance model developed here provides a simple explanation for why the carbon isotope signatures for 3HP/4HB pathway Sulfolobales and Thaumarchaeota are so different, despite both taxonomic groups of Archaea utilizing the same enzymatic pathway of autotrophic carbon fixation. The key observation is that the total biosynthetic isotope effect (ε_{Ar}) in Thaumarchaeota is larger than the probable magnitude of the isotope effect for the carbon-fixing enzyme (ε_{fix}). This requires that the substrate used for

carbon fixation (HCO_3^-) must itself be isotopically more negative than the extracellular supply. This internal disequilibrium manifests in the ammonia-oxidizing, marine Thaumarchaeota, but not in the aerobic, thermoacidophilic Sulfolobales, because all known members of the latter group contain carbonic anhydrase to facilitate intracellular HCO_3^- production. In contrast, the Thaumarchaeota apparently lack this capacity.

In addition to accurately reproducing the data for two specific prior studies (van der Meer et al., 2001a; Könneke et al., 2012), our model makes several testable predictions: the parameters as currently assigned in Table 1 predict a maximum dynamic range of *ca.* 5‰ for ε_{Ar} in modern marine environments, with maximum and minimum thresholds of *ca.* 23‰ and 18‰ (calculated relative to HCO_3^- - rather than DIC) for purely autotrophic metabolism. Values above 23‰ or below 18‰ either would require adjustment of model parameters, or would be interpreted, respectively, as indicating heterotrophic activity or active uptake of HCO_3^- by the marine Thaumarchaeota. Exploration of a variety of locations, sample types, and water chemistry conditions will help test these ranges, but data from our companion study of planktonic archaeal lipids from the Southwestern Atlantic Ocean water column are consistent with the present model (Hurley et al., 2019).

Considerable additional work is required, both at the cellular level and in environmental systems, to examine whether the ideas proposed here are consistent with additional observations and reproducible widely across taxa that fix carbon using the 3HP/4HB cycle. Laboratory cultures of *N. maritimus* to date have been grown at pH 7.5-7.6 in artificial seawater medium, leading to $[CO_{2(aq)}]$ values ≥ 40 μM, which is higher than most present-day upper ocean conditions *in situ*. Lower $[CO_{2(aq)}]$ levels should be tested experimentally. From sediments, core-top calibrations and examination of known pCO_2 excursions (*e.g.*, the most recent deglaciation) would be reasonable first steps. With further exploration, ε_{Ar} may prove useful for pCO_2 paleobarometry.

ACKNOWLEDGEMENTS

We thank Martin Könneke, Jed Fuhrman, David Johnston, Emma Bertran, Itay Halevy, Rich Pancost, and Anne Dekas for valuable discussions. We are grateful to Joe Werne for editorial assistance and to three anonymous reviewers for their valuable comments. Funding from NSF-1129343, NSF-1702262, and the

Gordon and Betty Moore Foundation (to A.P.); from National Science Foundation Graduate Research Fellowship DGE-1144152 (to E.B.W.); and from the Agouron Institute (to S.J.H.) supported this work.

REFERENCES

Adam, P.S., Borrel, G., Brochier-Armanet, C. and Gribaldo S. (2017) The growing tree of Archaea: new perspectives on their diversity, evolution and ecology. *ISME Journal* **11**, 2407-2425.

Albery, W. J., and Knowles, J. R. (1976) Evolution of enzyme function and the development of catalytic efficiency. *Biochemistry* **15**, 5631–5640.

Altschul, S.F., Madden, T.L., Schaffer, A.A., Zhang, J.H., Zhang, Z., Miller, W. and Lipman, D.J. (1997) Gapped BLAST and PSI-BLAST: a new generation of protein database search programs. *Nucleic Acids Research* **25**, 3389-3402.

Amenabar, M. J., Shock, E. L., Roden, E. E., Peters, J. W. and Boyd, E. S. (2017) Microbial substrate preference dictated by energy demand rather than supply. *Nature Geoscience* **10**, 577-581.

Auernik, K.S. and Kelly, R.M. (2010) Physiological Versatility of the Extremely Thermoacidophilic Archaeon Metallosphaera sedula Supported by Transcriptomic Analysis of Heterotrophic, Autotrophic, and Mixotrophic Growth. *Applied and Environmental Microbiology* **76**, 931-935.

Bar-Even, A., Noor, E., Savir, Y., Liebermeister, W., Davidi, D., Tawfik, D.S. and Milo, R. (2011) The moderately efficient enzyme: evolutionary and physicochemical trends shaping enzyme parameters. *Biochemistry* **50**, 4402-4410.

Bennett, B. D., Kimball, E. H., Gao, M., Osterhout, R., Van Dien, S. J., and Rabinowitz, J. D. (2009) Absolute metabolite concentrations and implied enzyme active site occupancy in *Escherichia coli*. *Nature Chemical Biology* **5**, 593–599.

Berg, I.A., Kockelkorn, D., Buckel, W. and Fuchs, G. (2007) A 3-hydroxypropionate/4-hydroxybutyrate autotrophic carbon dioxide assimilation pathway in archaea. *Science* **318**, 1782-1786.

Berg, I.A., Kockelkorn, D., Ramos-Vera, W.H., Say, R.F., Zarzycki, J., Hügler, M., Alber, B.E. and Fuchs, G. (2010) Autotrophic carbon fixation in archaea. *Nature Reviews Microbiology* **8**, 447–460.

Bidigare, R.R., Fluegge, A., Freeman, K.H., Hanson, K.L., Hayes, J.M., Hollander, D., Jasper, J.P., King, L.L., Laws, E.A., Milder, J., Millero, F.J., Pancost, R., Popp, B.N., Steinberg, P.A. and Wakeham, S.G. (1997) Consistent fractionation of C-13 in nature and in the laboratory: Growth-rate effects in some haptophyte algae. *Global Biogeochemical Cycles* **11**, 279-292.

Bundy H. F. (1986) Comparative kinetics and inhibition of a carbonic anhydrase from *Chlamydomonas reinhardii*. *Comp. Biochem. Physiol*. **84B**, 63-69.

Calvin, M. and Benson, A.A. (1948) The path of carbon in photosynthesis. *Science* **107**, 476-480.

Dekas, A.E., Parada, A.E., Mayali, X., Fuhrman, J.A., Weber, P.K. and Pett-Ridge, J. (2018) Investigating Organic Substrate Utilization by Marine Thaumarchaeota Using Metatranscriptomics and FISH-NanoSIMS. 2018 Ocean Sciences Meeting, Abstract D137.

Elling, F.J., Doeana, K.D., Gottschalk, J., Kusch, S., Hurley, S.J., Polik, C.A., Pearson, A. (2019) Archaeal lipid biomarker constraints on the carbon isotope excursion across the Paleocene-Eocene boundary. *Nature Communications, in review.*

Estelmann, S., Hügler, M., Eisenreich, W., Werner, K., Berg, I.A., Ramos-Vera, W.H., Say, R.F., Kockelkorn, D., Gad'on, N. and Fuchs, G. (2011) Labeling and Enzyme Studies of the Central Carbon Metabolism in Metallosphaera sedula. *Journal of Bacteriology* **193**, 1191-1200.

Evans, M.C.W., Buchanan, B.B. and Arnon, D.I. (1966) A new ferredoxin-dependent carbon reduction cycle in a photosynthetic bacterium. *Proceedings of the National Academy of Sciences of the United States of America* **55**, 928-.

Foster, G.L., Lear, C.H. and Rae J.W.B (2012) The evolution of pCO_2, ice volume and climate during the middle Miocene. *Earth and Planetary Science Letters* **341-344**, 243-254.

Greenop, R., Foster, G.L., Wilson, P.A. and Lear, C.H. (2014) Middle Miocene climate instability associated with high-amplitude CO2 variability. *Paleoceanography and Paleoclimatology* **29**, 845-853.

Guy, L. and Ettema, T.J.G. (2011) The archaeal 'TACK' superphylum and the origin of eukaryotes. *Trends in Microbiology* **19**, 580-587.

Hallam, S.J., Konstantinidis, K.T., Putnam, N., Schleper, C., Watanabe, Y., Sugahara, J., Preston, C., de la Torre, J., Richardson, P.M. and DeLong, E.F. (2006) Genomic analysis of the uncultivated marine crenarchaeote Cenarchaeum symbiosum. *Procoeedings of the National Academy of Sciences USA* **103**, 18296-18301.

Hawkins, A.B., Adams, M.W. and Kelly, R.M. (2014) Conversion of 4-hydroxybutyrate to acetyl coenzyme A and its anapleurosis in the *Metallosphaera sedula* 3-hydroxypropionate/4-hydroxybutyrate carbon fixation pathway. *Applied and Environmental Microbioilogy* **80**, 2536–2545.

Hayes, J.M. (1993) Factors controlling C-13 contents of sedimentary organic compounds – Principles and evidence. *Marine Geology* **113**, 111-125.

Hayes, J.M. (2001) Fractionation of carbon and hydrogen isotopes in biosynthetic processes, *Stable Isotope Geochemistry*, pp. 225-277.

Herndl, G.J., Reinthaler, T., Teira, E., van Aken, H., Veth, C., Pernthaler, A. and Pernthaler, J. (2005) Contribution of Archaea to total prokaryotic production in the deep Atlantic Ocean. *Applied and Environmental Microbiology* **71**, 2303-2309.

Hoefs, M.J.L., Schouten, S., deLeeuw, J.W., King, L.L., Wakeham, S.G. and Damste, J.S.S. (1997) Ether lipids of planktonic archaea in the marine water column. *Applied and Environmental Microbiology* **63**, 3090-3095.

Holo, H. and Sirevag, R. (1986) Autotrophic growth and CO_2 fixation of *Chloroflexus aurantiacus*. *Archives of Microbiology* **145**, 173-180.

Hopkinson B. M., Dupont C. L., Allen A. E., Morel F. M. M. (2011) Efficiency of the CO_2-concentrating mechanism of diatoms. *Procoeedings of the National Academy of Sciences USA* **108**, 3830–3837.

House, C.H., Schopf, J.W. and Stetter, K.O. (2003) Carbon isotopic fractionation by Archaeans and other thermophilic prokaryotes. *Organic Geochemistry* **34**, 345-356.

Huber, G., Spinnler, C., Gambacorta, A. and Stetter, K.O. (1989) *Metallosphaera sedula* gen. and sp. nov. represents a new genus of aerobic, metal-mobilizing, thermoacidophilic archaebacteria. *System. Appl. Microbiol.* **12**, 38-47.

Huber, H., Gallenberger, M., Jahn, U., Eylert, E., Berg, I.A., Kockelkorn, D., Eisenreich, W. and Fuchs, G. (2008) A dicarboxylate/4-hydroxybutyrate autotrophic carbon assimilation cycle in the hyperthermophilic Archaeum Ignicoccus hospitalis. *Proceedings of the National Academy of Sciences of the United States of America* **105**, 7851-7856.

Hug, L.A., Baker, B.J., Anantharaman, K., Brown, C.T., Probst, A.J., Castelle, C.J. et al. (2016). A new view of the tree of life. *Nature Microbiology* **1**, 16048.

Hügler, M., Krieger, R.S., Jahn, M. and Fuchs, G. (2003) Characterization of acetyl-CoA/propionyl-CoA carboxylase in Metallosphaera sedula - Carboxylating enzyme in the 3-hydroxypropionate cycle for autotrophic carbon fixation. *European Journal of Biochemistry* **270**, 736-744.

Hurley, S.J., Elling, F.J., Könneke, M., Buchwald, C., Wankel, S.D., Santoro, A.E., Lipp, J.S., Hinrichs, K.U. and Pearson, A. (2016) Influence of ammonia oxidation rate on thaumarchaeal lipid composition and the TEX86 temperature proxy. *Proceedings of the National Academy of Sciences of the United States of America* **113**, 7762-7767.

Hurley, S.J., Close, H.G., Elling, F.J., Jasper, C.E., Gospodinova, K., McNichol, A.P., Pearson, A. (2019) CO_2-dependent carbon isotope fractionation in Archaea, Part II: Natural marine planktonic populations., *Geochimica et Cosmochimica Acta*, *accepted.*

Ingalls, A.E., Shah, S.R., Hansman, R.L., Aluwihare, L.I., Santos, G.M., Druffel, E.R.M. and Pearson, A. (2006) Quantifying archaeal community autotrophy in the mesopelagic ocean using natural

radiocarbon. *Proceedings of the National Academy of Sciences of the United States of America* **103**, 6442-6447.

Iverson, V., Morris, R.M., Frazar, C.D., Berthiaume, C.T., Morales, R.L. and Armbrust, E.V. (2012) Untangling genomes from metagenomes: Revealing an uncultured class of marine Euryarchaeota. *Science* **335**, 587-590.

Jasper, J.P., Hayes, J.M., Mix, A.C. and Prahl, F.G. (1994) Photosynthetic fractionation of C-13 and concentrations of dissolved CO_2 in the Central Equatorial Pacific during the last 255,000 years. *Paleoceanography* **9**, 781-798.

Jennings, R.M., Whitmore, L.M., Moran, J.J., Kreuzer, H.W. and Inskeep, W.P. (2014) Carbon dioxide fixation by *Metallosphaera yellowstonensis* and acidothermophilic iron-oxidizing microbial communities from Yellowstone National Park. *Applied and Environmental Microbiology* **80**, 2665-2671.

Johnson, S.L. and Morrison, D.L. (1972) Kinetics and mechanism of decarboxylation of *N*-arylcarbamates. Evidence for kinetically important zwitterionic carbonic acid species of short lifetime. *Journal of the American Chemical Society* **94**, 1324-1334.

Keller, M. A., Piedrafita G., and Ralser M. (2015) The widespread role of non-enzymatic reactions in cellular metabolism. *Curr. Opin. Biotech.* **34**, 153-161.

Kerou, M., Offre, P., Valledor, L., Abby, S.S., Melcher, M., Nagler, M., Weckwerth, W. and Schleper C. (2016) Proteomics and comparative genomics of *Nitrososphaera viennensis* reveal the core genome and adaptations of archaeal ammonia oxidizers. *Proceedings of the National Academy of Sciences of the United States of America* **113**, E7937-E7946.

Kim, J.G., Park, S.J., Damste, J.S.S., Schouten, S., Rijpstra, W.I.C., Jung, M.Y., Kim, S.J., Gwak, J.H., Hong, H., Si, O.J., Lee, S., Madsen, E.L. and Rhee, S.K. (2016) Hydrogen peroxide detoxification is a key mechanism for growth of ammonia-oxidizing archaea. *Proceedings of the National Academy of Sciences of the United States of America* **113**, 7888-7893.

Klawonn, I., Nahar, N., Walve, J., Andersson, B., Olofsson, M., Svedén, J.B., Littmann, S., Whitehouse, M.J., Kuypers, M.M. and Ploug, H. (2016) Cell-specific nitrogen- and carbon-fixation of cyanobacteria in a temperate marine system (Baltic Sea). *Environmental Microbiology* **18**, 4596-4609.

Könneke, M., Bernhard, A.E., de la Torre, J.R., Walker, C.B., Waterbury, J.B. and Stahl, D.A. (2005) Isolation of an autotrophic ammonia-oxidizing marine archaeon. *Nature* **437**, 543-546.

Könneke, M., Lipp, J.S. and Hinrichs, K.U. (2012) Carbon isotope fractionation by the marine ammonia-oxidizing archaeon Nitrosopumilus maritimus. *Organic Geochemistry* **48**, 21-24.

Könneke, M., Schubert, D.M., Brown, P.C., Hügler, M., Standfest, S., Schwander, T., von Borzyskowski, L.S., Erb, T.J., Stahl, D.A. and Berg, I.A. (2014) Ammonia-oxidizing archaea use the most energy-efficient aerobic pathway for CO_2 fixation. *Proceedings of the National Academy of Sciences of the United States of America* **111**, 8239-8244.

Kuypers, M.M.M., Blokker, P., Erbacher, J., Kinkel, H., Pancost, R.D., Schouten, S. and Damste, J.S.S. (2001) Massive expansion of marine archaea during a mid-Cretaceous oceanic anoxic event. *Science* **293**, 92-94.

Lengger, S.K., Lipsewers, Y.A., de Haas, H., Sinninghe Damsté, J.S. and Schouten, S. (2014) Lack of ^{13}C-label incorporation suggests low turnover rates of thaumarchaeal intact polar tetraether lipids in sediments from the Iceland shelf. *Biogeosciences* **11**, 201-216.

Lever, M.A., Rogers, K.L., Lloyd, K.G., Overmann, J., Schink, B., Thauer, R.K., Hoehler, T.M. and Jorgensen, B.B. (2015) Life under extreme energy limitation: a synthesis of laboratory- and field-based investigations. *FEMS Microbiology Reviews* **39**, 688-728.

Lian, H., Zeldes, B.M., Lipscomb, G.L., Hawkins, A.B., Han, Y.J., Loder, A.J., Nishiyama, D., Adams, M.W.W. and Kelly, R.M. (2016) Ancillary contributions of heterologous biotin protein ligase and carbonic anhydrase for CO_2 incorporation into 3-hydroxypropionate by metabolically engineered Pyrococcus furiosus. *Biotechnology and Bioengineering* **113**, 2652-2660.

Loder, A.J., Han, Y.J., Hawkins, A.B., Lian, H., Lipscomb, G.L., Schut, G.J., Keller, M.W., Adams, M.W.W. and Kelly, R.M. (2016) Reaction kinetic analysis of the 3-hydroxypropionate/4-hydroxybutyrate CO2 fixation cycle in extremely thermoacidophilic archaea. *Metabolic Engineering* **38**, 446-463.

Loferer-Krössbacher, M., Klima, J., and Psenner, R. (1998) Determination of bacterial cell dry mass by transmission electron microscopy and densitometric image analysis. *Applied and Environmental Microbiology*. **64**, 688-694.

Martens-Habbena, W., Berube, P.M., Urakawa, H., de la Torre, J.R. and Stahl, D.A. (2009) Ammonia oxidation kinetics determine niche separation of nitrifying Archaea and Bacteria. *Nature* **461**, 976-U234.

McMurtrey, R.J. (2016) Analytic models of oxygen and nutrient diffusion, metabolism dynamics, and architecture optimization in three-dimensional tissue constructs with applications and insights in cerebral organoids. *Tissue Engineering* **22**, 221-249.

McNevin, D.B., Badger, M.R., Kane, H.J. and Farquhar, G.D. (2006) Measurement of (carbon) kinetic isotope effect by Rayleigh fractionation using membrane inlet mass spectrometry for CO_2-consuming reactions. *Functional Plant Biology* **33**, 1115-1128.

Menendez, C., Bauer, Z., Huber, H., Gad'on, N., Stetter, K.O. and Fuchs, G. (1999) Presence of acetyl coenzyme A (CoA) carboxylase and propionyl-CoA carboxylase in autotrophic Crenarchaeota and indication for operation of a 3-hydroxypropionate cycle in autotrophic carbon fixation. *Journal of Bacteriology* **181**, 1088-1098.

Mook, W.G., Bommerson, J.C. and Staverman, W.H. (1974) Carbon isotope fractionation between dissolved bicarbonate and gaseous carbon dioxide. *Earth and Planetary Science Letters* **22**, 169-176.

Offre, P., Kerou, M., Spang, A. and Schleper, C. (2014) Variabiligy of the transporter gene complement in ammonia-oxidizing archaea. *Trends in Microbiology* **22**, 665-675.

O'Leary, M.H., Rife, J.E. and Slater, J.D. (1981) Kinetic and isotope effect studies of maize phosphoenolpyruvate carboxylase. *Biochemistry* **20**, 7308-7314.

O'Leary, M.H. (1982) Phosophoenolpyruvate carboxylase: An enzymologist's view. *Annual Reviews Plant Physiology* **33**, 294-315.

Ouverney, C.C. and Fuhrman, J.A. (2000) Marine planktonic Archaea take up amino acids. *Applied and Environmental Microbiology* **66**, 4829-.

Pagani, M., Zachos, J.C., Freeman, K.H., Tipple, B. and Bohaty, S. (2005) Marked decline in atmospheric carbon dioxide concentrations during the Paleogene. *Science* **309**, 600-603.

Pancost, R.D., Coleman, J.M., Love, G.D., Chatzi, A., Bouloubassi, I. and Snape, C.E. (2008) Kerogen-bound glycerol dialkyl tetraether lipids released by hydropyrolysis of marine sediments: A bias against incorporation of sedimentary organisms? *Organic Geochemistry* **39**, 1359-1371.

Pancost, R.D., Hopmans, E.C., Damste, J.S.S. and Party, M.S.S. (2001) Archaeal lipids in Mediterranean cold seeps: Molecular proxies for anaerobic methane oxidation. *Geochimica et Cosmochimica Acta* **65**, 1611-1627.

Paneth, P. and O'Leary, M.H. (1985) Carbon isotope effect on dehydration of bicarbonate ion catalyzed by carbonic anhydrase. *Biochemistry* **24**, 5143–5147.

Pearson, A., Hurley, S.J., Walter, S.R.S., Kusch, S., Lichtin, S. and Zhang, Y.G. (2016) Stable carbon isotope ratios of intact GDGTs indicate heterogeneous sources to marine sediments. *Geochimica et Cosmochimica Acta* **181**, 18-35.

Pearson, A., McNichol, A.P., Benitez-Nelson, B.C., Hayes, J.M. and Eglinton, T.I. (2001) Origins of lipid biomarkers in Santa Monica Basin surface sediment: A case study using compound-specific Delta C-14 analysis. *Geochimica et Cosmochimica Acta* **65**, 3123-3137.

Peeples, T.L. and Kelly, R.M. (1995) Bioenergetic response of the extreme thermoacidophile *Metallosphaera sedula* to thermal and nutritional stresses. *Applied and Environmental Microbiology* **61**, 2314-2321.

Pester, M., Schleper, C. and Wagner, M. (2011) The Thaumarchaeota: an emerging view of their phylogeny and ecophysiology. *Current Opinion in Microbiology* **14**, 300-306.

Polik, C.A., Elling, F.J. and Pearson, A. (2018) Impacts of paleoecology on the TEX_{86} sea surface temperature proxy in the Pliocene-Pleistocene Mediterranean Sea. (Paleoceanography and Paleoclimatology, *doi.org/10.1029/2018PA003494.*

Qin, W., Amin, S.A., Lundeen, R.A., Heal, K.R., Martens-Habbena, W., Turkarslan, S., Urakawa, H., Costa, K.C., Hendrickson, E.L., Wang, T., Beck, D.A.C., Tiquia-Arashiro, S.M., Taub, F., Holmes, A.D., Vajrala, N., Berube, P.M., Lowe, T.M., Moffett, J.W., Devol, A.H., Baliga, N.S., Arp, D.J., Sayavedra-Soto, L.A., Hackett, M., Armbrust, E.V., Ingalls, A.E. and Stahl, D.A. (2018) Stress response of a marine ammonia-oxidizing archaeon informs physiological status of environmental populations. *ISME Journal* **12**, 508-519.

Qin, W., Amin, S.A., Martens-Habbena, W., Walker, C.B., Urakawa, H., Devol, A.H., Ingalls, A.E., Moffett, J.W., Armbrust, E.V. and Stahl, D.A. (2014) Marine ammonia-oxidizing archaeal isolates display obligate mixotrophy and wide ecotypic variation. *Proceedings of the National Academy of Sciences of the United States of America* **111**, 12504-12509.

Rau, G.H., Takahashi, T., Desmarais, D.J., Repeta, D.J. and Martin, J.H. (1992) The relationship between $\delta^{13}C$ of organic matter and $CO_2(aq)$ in ocean surface water – Data from a JGOFS site in the Northeast Atlantic Ocean and a model. *Geochimica et Cosmochimica Acta* **56**, 1413-1419.

Royer, D.L., Berner, R.A. and Beerling, D.J. (2001) Phanerozoic atmospheric CO_2 change: Evaluating geochemical and paleobiological approaches. *Earth-Science Reviews* **54**, 349-392.

Santoro, A. E. and Casciotti, K. L. (2011) Enrichment and characterization of ammonia-oxidizing archaea from the open ocean: phylogeny, physiology and stable isotope fractionation. *ISME Journal* **5**, 1796–1808.

Santoro, A.E., Dupont, C.L., Richter, R.A., Craig, M.T., Carini, P., McIlvin, M.R., Yang, Y., Orsi, W.D., Moran, D.M. and Saito, M.A. (2015) Genomic and proteomic characterization of "Candidatus Nitrosopelagicus brevis": An ammonia-oxidizing archaeon from the open ocean. *Proceedings of the National Academy of Sciences of the United States of America* **112**, 1173-1178.

Schoon, P.L., Heilmann-Clausen, C., Schultz, B.P., Sluijs, A., Damste, J.S.S. and Schouten, S. (2013) Recognition of Early Eocene global carbon isotope excursions using lipids of marine Thaumarchaeota. *Earth and Planetary Science Letters* **373**, 160-168.

Schouten, S., Hopmans, E.C. and Damste, J.S.S. (2013) The organic geochemistry of glycerol dialkyl glycerol tetraether lipids: A review. *Organic Geochemistry* **54**, 19-61.

Schouten, S., Hopmans, E.C., Schefuss, E. and Damste, J.S.S. (2002) Distributional variations in marine crenarchaeotal membrane lipids: a new tool for reconstructing ancient sea water temperatures? *Earth and Planetary Science Letters* **204**, 265-274.

Schouten, S., Middelburg, J.J., Hopmans, E.C. and Damste, J.S.S. (2010) Fossilization and degradation of intact polar lipids in deep subsurface sediments: A theoretical approach. *Geochimica et Cosmochimica Acta* **74**, 3806-3814.

Schubotz, F., Lipp, J.S., Elvert, M. and Hinrichs, K.U. (2011) Stable carbon isotopic compositions of intact polar lipids reveal complex carbon flow patterns among hydrocarbon degrading microbial communities at the Chapopote asphalt volcano. *Geochimica et Cosmochimica Acta* **75**, 4399-4415.

Sessions, A.L., Sylva, S.P. and Hayes, J.M. (2005) Moving-wire device for carbon isotopic analyses of nanogram quantities of nonvolatille organic carbon. *Analytical Chemistry* **77**, 6519-6527.

Seyler, L.M., McGuinness, L.R., Gilbert, J.A., Biddle, J.F. and Kerkhof, L.J. (2018) Discerning autotrophy, mixotrophy and heterotrophy in marine TACK archaea from the North Atlantic.*FEMS Microbiology Ecology* **94**, fiy014.

Shah, S.R., Mollenhauer, G., Ohkouchi, N., Eglinton, T.I. and Pearson, A. (2008) Origins of archaeal tetraether lipids in sediments: Insights from radiocarbon analysis. *Geochimica et Cosmochimica Acta* **72**, 4577-4594.

Sirevag, R., Buchanan, B.B., Berry, J.A. and Troughton, J.H. (1977) Mechanisms of CO_2 fixation in bacterial photosynthesis studied by carbon isotope fractionation technique. *Archives of Microbiology* **112**, 35-38.

Smith, K.S. and Ferry, J.G. (1999) A plant type (β class) carbonic anhydrase from the thermophilic methanoarchaeon *Methanobacterium thermoautotrophicum*. *Journal of Bacteriology* **181**, 6247-6253.

Smith, K.S. and Ferry, J.G. (2000) Prokaryotic carbonic anhydrases. *FEMS Microbiology Reviews* **24**, 335-366.

Smith, K.S., Jakubzick, C., Whittam, T.S. and Ferry, J.G. (1999) Carbonic anhydrase is an ancient enzyme widespread in prokaryotes. *Proceedings of the National Academy of Sciences of the United States of America* **96**, 15184-15189.

Smittenberg, R.H., Hopmans, E.C., Schouten, S., Hayes, J.M., Eglinton, T.I. and Damste, J.S.S. (2004) Compound-specific radiocarbon dating of the varved Holocene sedimentary record of Saanich Inlet, Canada. *Paleoceanography* **19**, PA2012, doi:10.1029/2003PA000927.

Spang, A., Hatzenpichler, R., Brochier-Armanet, C., Rattei, T., Tischler, P., Spieck, E., Streit, W., Stahl, D. A., Wagner, M. and Schleper, C. (2010) Distinct gene set in two different lineages of ammonia-oxidizing archaea supports the phylum Thaumarchaeota. *Trends Microbiol* **18**, 331–340.

Stieglmeier, M., Klingl, A., Alves, R.J., Rittmann, S.K., Melcher, M., Leisch, N. and Schleper, C. (2014) *Nitrososphaera viennensis* gen. nov., sp. nov., an aerobic and mesophilic, ammonia-oxidizing archaeon from soil and a member of the archaeal phylum Thaumarchaeota. *International Journal of Systematic and Evolutionary Microbiology* **64**, 2738-2752.

Strauss, G. and Fuchs, G. (1993) Enzymes of a novel CO_2 fixation pathway in the phototrophic bacterium *Chloroflexus aurantiacus* – The 3-hydroxypropionate cycle. *European Journal of Biochemistry* **215**, 633-643.

Tang, T., Mohr, W., Sattin, S.R., Rogers, D.R., Girguis, P.R. and Pearson, A. (2017) Geochemically distinct carbon isotope distributions in *Allochromatium vinosum* DSM 180(T) grown photoautotrophically and photoheterotrophically. *Geobiology* **15**, 324-339.

Taylor, K.W.R., Huber, M., Hollis, C.J., Hernandez-Sanchez, M.T. and Pancost, R.D. (2013) Re-evaluating modern and Palaeogene GDGT distributions: Implications for SST reconstructions. *Global and Planetary Change* **108**, 158-174.

Tcherkez, G.G.B., Farquhar, G.D. and Andrews T.J. (2006) Despite slow catalysis and confused substrate specificity, all ribulose bisphosphate carboxylases may be nearly perfectly optimized. *Proceedings of the National Academy of Sciences USA* **103**, 7246-7251.

Tourna, M., Stieglmeier, M., Spang, A., Könneke, M., Schintlmeister, A., Urich, T., Engel, M., Schloter, M., Wagner, M., Richter, A. and Schleper, C. (2011) *Nitrososphaera viennensis*, an ammonia oxidizing archaeon from soil. *Proceedings of the National Academy of Sciences of the United States of America* **108**, 8420-8425.

Valentine, D.L. (2007) Adaptations to energy stress dictate the ecology and evolution of the Archaea. *Nature Reviews Microbiology* **5**, 316-323.

van der Meer, M.T.J., Schouten, S., Damste, J.S.S., de Leeuw, J.W. and Ward, D.M. (2003) Compound-specific isotopic fractionation patterns suggest different carbon metab lisms among Chloroflexus-like bacteria in hot-spring microbial mats. *Applied and Environmental Microbiology* **69**, 6000-6006.

van der Meer, M.T.J., Schouten, S., Rijpstra, W.I.C., Fuchs, G. and Damste, J.S.S. (2001a) Stable carbon isotope fractionations of the hyperthermophilic crenarchaeon *Metallosphaera sedula*. *FEMS Microbiology Letters* **196**, 67-70.

van der Meer, M.T.J., Schouten, S., van Dongen, D.E., Rijpstra, W.I.C., Fuchs, G., Damste, J.S.S., de Leeuw, J.W. and Ward, D.M. (2001b) Biosynthetic controls an the ^{13}C contents of organic components in the photoautotrophic bacterium *Chloroflexus aurantiacus*. *Journal of Biological Chemistry* **276**, 10971-10976.

Walker, C.B., de la Torre, J.R., Klotz, M.G., Urakawa, H., Pinel, N., Arp, D.J., Brochier-Armanet, C., Chain, P.S.G., Chan, P.P., Gollabgir, A., Hemp, J., Hügler, M., Karr, E.A., Könneke, M., Shin, M., Lawton, T.J., Lowe, T., Martens-Habbena, W., Sayavedra-Soto, L.A., Lang, D., Sievert, S.M., Rosenzweig, A.C., Manning, G. and Stahl, D.A. (2010) *Nitrosopumilus maritimus* genome reveals unique mechanisms for nitrification and autotrophy in globally distributed marine crenarchaea. *Proceedings of the National Academy of Sciences of the United States of America* **107**, 8818-8823.

Williams, T.A., Szöllősi, G.J., Spang, A., Foster, P.G., Heaps, S.E., Boussau, B. et al. (2017) Integrative modeling of gene and genome evolution roots the archaeal tree of life. *Proceedings of the National Academy of Sciences USA* **114**, E4602–E4611.

Wood, H.G., Ragsdale, S.W. and Pezacka, E. (1986) The acetyl-CoA pathway of autotrophic growth. *FEMS Microbiology Letters* **39**, 345-362.

Wuchter, C., Schouten, S., Boschker, H.T.S. and Damste, J.S.S. (2003) Bicarbonate uptake by marine Crenarchaeota. *FEMS Microbiology Letters* **219**, 203-207.

Xie, S., Lipp, J.S., Wegener, G., Ferdelman, T.G. and Hinrichs, K.-U. (2013) Turnover of microbial lipids in the deep biosphere and growth of benthic archaeal populations. *Proceedings of the National Academy of Sciences of the United States of America* **110**, 6010-6014.

Zeebe, R.E. (2014) Kinetic fractionation of carbon and oxygen isotopes during hydration of carbon dioxide. *Geochimica et Cosmochimica Acta* **139**, 540-552.

Zeebe, R.E. and Wolf-Gladrow, D.A. (2001) CO_2 in seawater: equilibrium, kinetics, isotopes. Amsterdam: Elsevier Science B.V.

Zhang, Y.G., Zhang, C.L.L., Liu, X.L., Li, L., Hinrichs, K.U. and Noakes, J.E. (2011) Methane Index: A tetraether archaeal lipid biomarker indicator for detecting the instability of marine gas hydrates. *Earth and Planetary Science Letters* **307**, 525-534.

Zhang, Y.G., Pagani, M., Liu, Z., Bohaty, S.M. and DeConto, R. (2013) A 40-million-year history of atmospheric CO_2. *Philosophical Transactions of the Royal Society A* **371**, 20130096.

Zeebe, R.E. and Wolf-Gladrow, D.A. (2001) CO_2 in seawater: equilibrium, kinetics, isotopes. Amsterdam: Elsevier Science B.V.

Table 1. Inputs and solutions for the simplified model (Figure 1a).

	Parameter	Units	*M. sedula*	Refs., Notes	*N. maritimus*	Refs., Notes
Cell Properties						
Length	L	μm	*n/a*		0.7	*1,2*
Radius	r_0	μm	0.5	*3*	0.1	*1,2*
Volume		μm^3	0.52		0.022	
C content	Bio	fgC $cell^{-1}$	120	*4*	10	*4, 5, 6*
C density	ρ	fmolC μm^{-3}	19.1		37.9	
Total protein	γBio	fgC $cell^{-1}$	96	*a*	8	*a*
Doubling time	T_d	hr	10	*7, 8, b*	34, various*	*9, 10*
Growth rate	μ	s^{-1}	1.93E-05		5.66E-06, various	
C-fix rate	fix	amolC μm^{-3} s^{-1}	0.37	*c*	0.21, various	*c*
C-fix activity	A	nmolC min^{-1} mg^{-1}	120	*7*	27	*6*
Growth Medium						
pH			2.0	*11*	7.5-7.6, various	*6, 9, 10, d*
pCO_2		atm	1.17	*11*		
[DIC]		mM			2.0	*9, 10*
$[CO_2(aq)]$	C_e	amol μm^{-3} (mM)	18.4	*e*	0.039, various	*e*
$[HCO_3^-]$	H_e	amol μm^{-3} (mM)	0.0025	*e*	1.9	*e*
Intracellular Conditions						
pH			5.4, 6.3**	*12, f*	*n/a*, 7.2**	*f*
$[CO_2(aq)]$	C_i	amol μm^{-3} (mM)	18.4	*e, g*	0.039, various	*e, h*
Acetyl/Propionyl-CoA Carboxylase Properties						
ACC complex		kDa	560	*7*	560	*i*
ACC fraction of cell			0.02	*7, 13, j*	0.01	*14*
ACC concentration	E_{fix}	mM	0.014		0.013	
k_{cat}	k_{cat2}	s^{-1}	28	*7*	280	*k*
K_M	K_{M2}	mM	0.3		0.03	*k*
k_{cat}/K_M, HCO_3^- fixation		amol μm^{-3} s^{-1}	93		9300	*l*
Carbonic Anhydrase (or HYD) Properties						
CA or HYD concentration	E_1	mM	0.014	*m*	0.014, various	*m, n*
k_{cat}	k_{cat1}	s^{-1}	10000	*15*	30	
K_M	K_{M1}	mM	2	*15*	0.003	*o*
k_{cat}/K_M, CO_2 hydration		amol μm^{-3} s^{-1}	5000		10000	*p*
Isotopic Inputs						
$\delta^{13}C$, $CO_2(aq)$	$\delta C_e = \delta C_i$	‰	-43.1	*11*	-15.4	*9, e*
$\delta^{13}C$, HCO_3^-	δH_e	‰	-38.0	*11*	-6.8	*9, e*
KIE, CO_2 hydration	ε_{CA}, ε_{HYD}	‰	1	*16*	25	*17*
$CO_2 \leftrightarrow HCO_3^-$ equilibrium	$\alpha_{CO2\text{-}HCO3\text{-}}$		0.995	*18, q*	0.991	*18, q*
KIE, ACC	ε_{fix}	‰	2.5	*19, r*	2.5	*19, r*
Flux and Isotopic Solutions						
CO_2 hydration rate	φ_4	amol μm^{-3} s^{-1}	124.0		0.402	
HCO_3^- dehydration rate	φ_5	amol μm^{-3} s^{-1}	123.7		0.187	
$[HCO_3^-]$ (intracellular)	H_i	amol μm^{-3} (mM)	6.3		0.0019	
dehydration ratio	$B = \varphi_5/\varphi_4$		> 0.99		0.47	
$\delta^{13}C$, HCO_3^-	δH_i	‰	-38.1		-23.4	
$\delta^{13}C$, Biomass	$\delta_{biomass}$	‰	-40.6		-25.9	
$\Delta\delta(HCO_3^-\text{-Bio})$, vs. H_e		‰	2.5		19.1	
$\varepsilon(HCO_3^-\text{-Bio})$ vs. H_e	ε_{Ar}	‰	2.6		19.6	
$\delta^{13}C$, Biomass, error	err	‰	-0.4		0.4	

*Values of T_d, *fix*, pH, $[CO_{2(aq)}]$ and E_1 were varied to test the model sensitivity. **First listed value is from the literature, while the second value reflects the model outcome; *n/a*, no estimate of intracellular pH for *N. maritimus* is available. **References.** *1*, Könneke et al., 2012; *2*, Santoro et al., 2015; *3*, Huber et al., 1989; *4*, Loferer-Krossbacher et al., 1998; *5*, Martens-Habbena et al., 2009; *6*, Könneke et al., 2014; *7*, Hügler et al., 2003; *8*, Menendez et al., 1999; *9*, Könneke et al., 2012; *10*, Hurley et al., 2016; *11*, van der Meer et al., 2001a; *12*, Peeples and Kelly, 1995; *13*, Lian et al., 2016; *14*, Qin et al., 2018; *15*, Smith and Ferry, 2000; *16*, Paneth and O'Leary, 1985; *17*, Zeebe, 2014;*18*, Mook et al., 1974; *19*, McNevin et al., 2006. **Notes.** Notes *a-r* appear in Supplemental Information.

FIGURE CAPTIONS

Figure 1. **(a)** Simplified analytical and **(b)** full numerical 3HP/4HB flux-balance models. **Carbon pools**: C*e*, external [$CO_{2(aq)}$]; C_i, internal[$CO_{2(aq)}$]; H_e, external [HCO_3^-], H_i, internal [HCO_3^-]; U, urea or other LMW organic metabolites metabolized to CO_2; Bio, total cell biomass. **Fluxes**: φ_1, diffusion of CO_2 into the cell; φ_2, diffusion of CO_2 out of the cell; φ_3, CO_2 derived from metabolism of organic substances; φ_4, hydration of CO_2 → HCO_3^-; φ_5, dehydration of HCO_3^- → CO_2; φ_6, active import of HCO_3^-; φ_7, diffusive leakage of HCO_3^- (as H_2CO_3; Mangan et al., 2016); *fix*, autotrophic carbon fixation rate. *N. maritimus* is rod-shaped, while *M. sedula* is coccoid. The simplified version assumes φ_3, φ_6, and φ_7 are zero.

Figure 2. **(a)** Solution to the simplified flux-balance model. Widths of arrows highlight the flux magnitudes for intracellular $C_i \Leftrightarrow H_i$ interconversion, normalized to carbon fixation (*fix*, Table 1). **(b), (c)** Relative $\delta^{13}C$ values for intracellular and extracellular carbon pools in the *M. sedula* and *N. maritimus* simple models (vertical axis not to scale). In both **b** and **c**, ε_{Ar} reflects the difference between $\delta_{biomass}$ and the external environment (δ_{He}). **(d)** Illustration of the relationship between dehydration ($B = \varphi_5/\varphi_4$) ratio and ε_{Ar}. When *B* approaches 1, as for *M. sedula*, H_i is in equilibrium and ε_{Ar} approaches ε_{fix}, regardless of the KIE chosen for ε_{CA} or ε_{HYD}. For *N. maritimus*, neither ε_{HYD} nor *B* is known uniquely, but the maximum allowed value of *B* is 0.47 (assuming ε_{HYD} is not larger than the 25‰ KIE for abiotic hydration); in the limit of B → 0, ε_{HYD} cannot be < 11‰.

Figure 3. Predicted response of ε_{Ar} to [$CO_{2(aq)}$] and μ (expressed as doubling time, T_d) for *N. maritimus*. The enzymatic parameters that affect these results currently are based on assumptions (Table 1); the values are optimized to reproduce existing $\delta^{13}C$ data for *N. maritimus* (Könneke et al., 2012), for marine Thaumarchaeota more generally (Schouten et al., 2013; Pearson et al., 2016), and to agree with an existing data set for marine POM (Hurley et al., 2019).

Figure 4. Sensitivity of the *N. maritimus* numerical model (Fig. 1b) to HCO_3^- import and incorporation of respiratory CO_2 (including from urea metabolism). Solid lines show HCO_3^- (H) import equivalent to 0, 10, or 20% of total carbon fixation (*fix*); dashed lines show incorporation of respiratory CO_2 (U, urea) at 60% of *fix*. Endmember values of δ_{He} and δ_U were +1‰ and -23‰, respectively. A slow generation time (T_d = 96 hr) moderately diminishes the effects of the H and U fluxes. The intersection of the observed ε_{Ar} and the H = 0% curves at >30 μM C_e and a 34-hour doubling time (T_d) reflects the behavior of the low-pH cultures of Könneke et al. (2012), while the 96-hour doubling time reflects the observations from marine POM (Hurley et al., 2019).

Figure 5. Predicted sensitivity of the ε_{Ar} proxy to changes in atmospheric pCO_2 and three different doubling times (T_d) for archaeal growth. Curves are calculated based on 15°C seawater, pH 8.0, a temperature-sensitive Henry's Law constant (Zeebe and Wolf-Gladrow, 2001), and assuming equilibrium partitioning. Shaded areas indicate the uncertainty in reconstructed pCO_2 values that would result from analytical precision of ±0.2‰. Most records would be accompanied by errors due to uncertainty in reconstructing δ_{He}, implying that uncertainties of +200/-100 ppm at 1000-ppm pCO_2 represent the best-case scenario.

Figure 1.

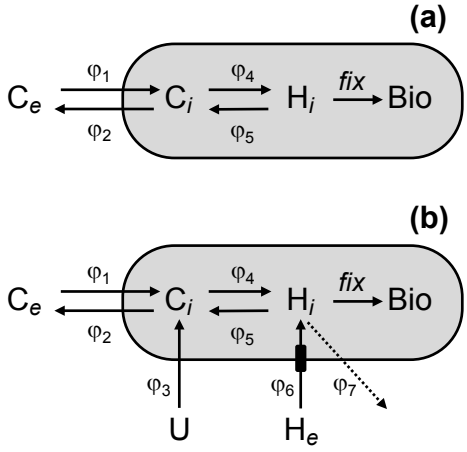

Figure 2.

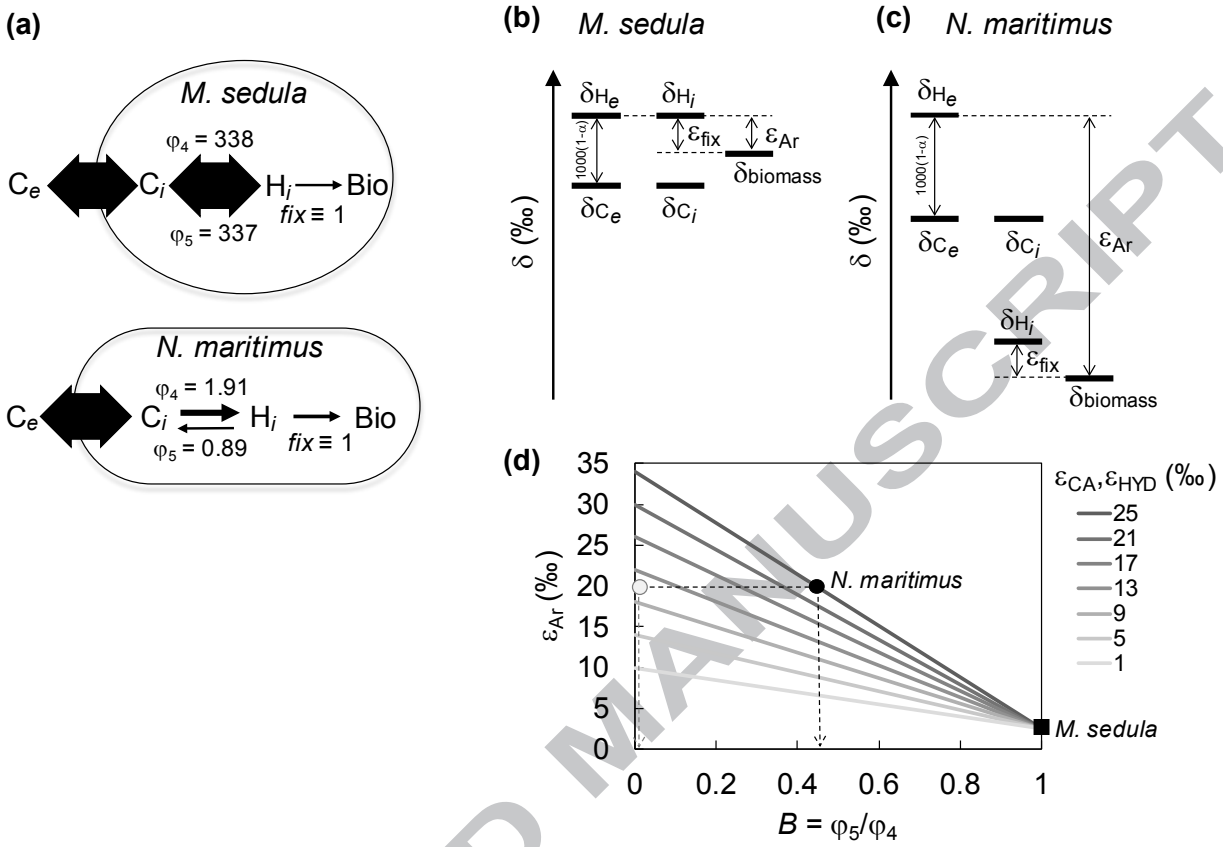

Figure 3.

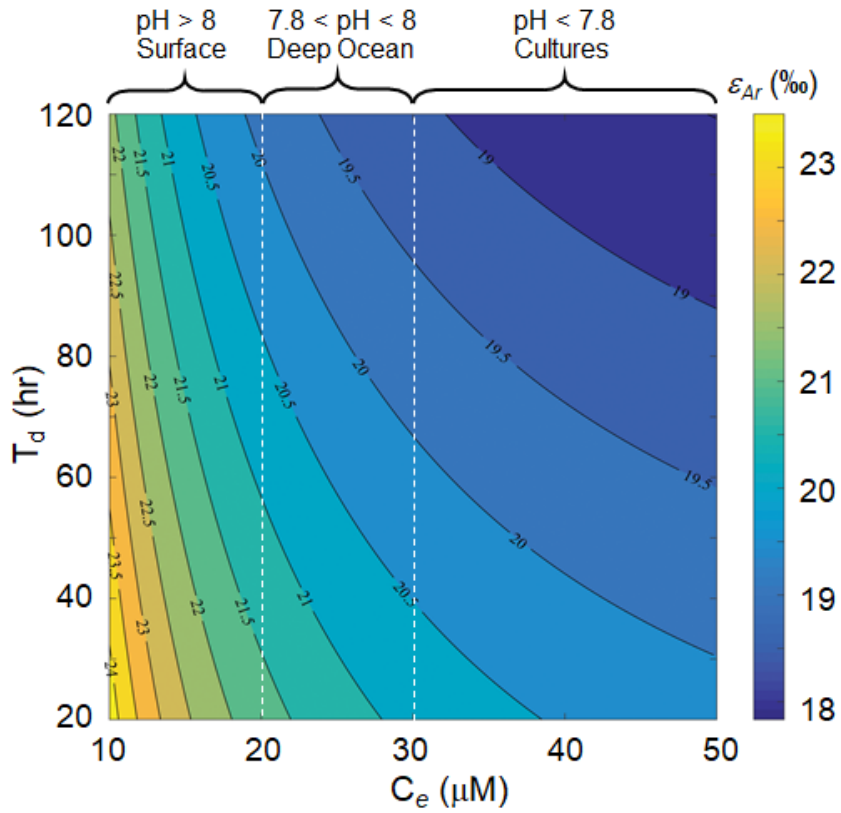

Figure 4.

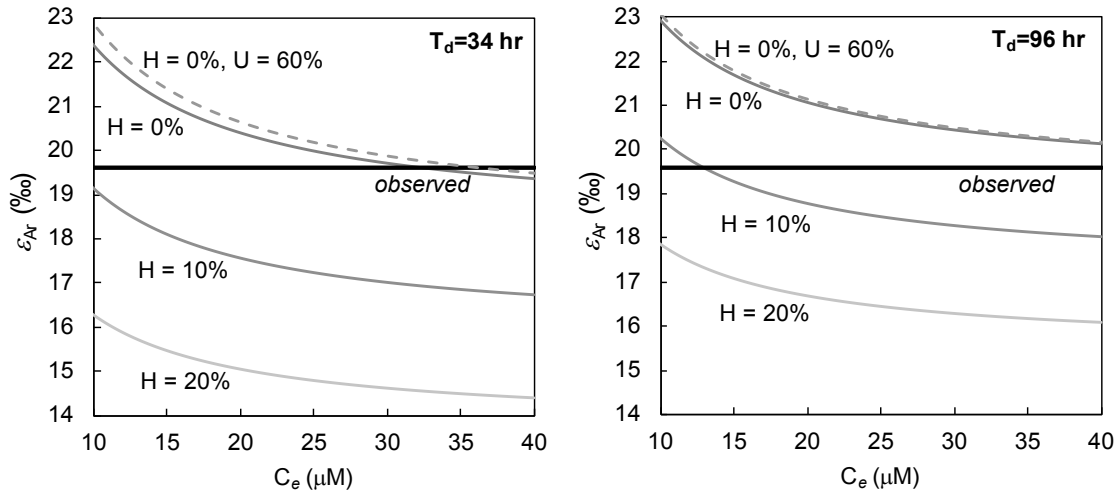

Figure 5.